Title: Biocompatibile microemulsions of a model nsaid for skin delivery: A decisive role of surfactants in skin penetration/irritation profiles and pharmacokinetic performance

Author: Marija N. Todosijević Miroslav M. Savić Bojan B. Batinić Bojan D. Marković Mirjana Gašperlin Danijela V. Randelović Milica Ž. Lukić Snežana D. Savić

PII: S0378-5173(15)30314-8
DOI: http://dx.doi.org/doi:10.1016/j.ijpharm.2015.10.048
Reference: IJP 15303

To appear in: *International Journal of Pharmaceutics*

Received date: 28-7-2015
Revised date: 15-10-2015
Accepted date: 16-10-2015

Please cite this article as: Todosijević, Marija N., Savić, Miroslav M., Batinić, Bojan B., Marković, Bojan D., Gašperlin, Mirjana, Ran*DF*elović, Danijela V., Lukić, Milica Ž., Savić, Snežana D., Biocompatibile microemulsions of a model nsaid for skin delivery: A decisive role of surfactants in skin penetration/irritation profiles and pharmacokinetic performance.International Journal of Pharmaceutics http://dx.doi.org/10.1016/j.ijpharm.2015.10.048

BIOCOMPATIBILE MICROEMULSIONS OF A MODEL NSAID FOR SKIN DELIVERY: A DECISIVE ROLE OF SURFACTANTS IN SKIN PENETRATION/IRRITATION PROFILES AND PHARMACOKINETIC PERFORMANCE

Marija N. Todosijević[1], Miroslav M. Savić[2], Bojan B. Batinić[2], Bojan D. Marković[3], Mirjana Gašperlin[4], Danijela V. Ranđelović[5], Milica Ž. Lukić[1], Snežana D. Savić[1*]

snexs@pharmacy.bg.ac.rs

[1]Department of Pharmaceutical Technology and Cosmetology, Faculty of Pharmacy, University of Belgrade, 11221 Belgrade, Serbia

[2]Department of Pharmacology, Faculty of Pharmacy, University of Belgrade, 11221 Belgrade, Serbia

[3]Department of Pharmaceutical Chemistry, Faculty of Pharmacy, University of Belgrade, 11221 Belgrade, Serbia

[4]Department of Pharmaceutical Technology, Faculty of Pharmacy, University of Ljubljana, 1000 Ljubljana, Slovenia

[5]ICTM – Institute of Microelectronic Technologies, University of Belgrade, 11000 Belgrade, Serbia

[*]Corresponding author at: Department of Pharmaceutical Technology and Cosmetology, Faculty of Pharmacy, University of Belgrade, Vojvode Stepe 450, 11221 Belgrade, Serbia. Tel.: +381113951366; Fax: +381113972840.

Graphical abstract

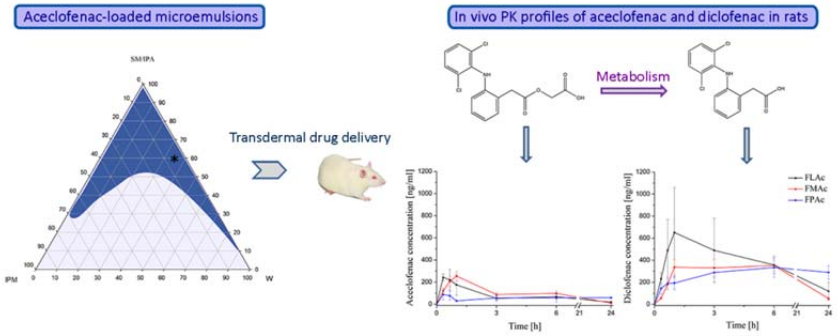

Abstract

To elaborate the decisive role of surfactants in promotion of aceclofenac' skin absorption, potentially avoiding irritation, we developed non-ionic microemulsions varying natural or synthetic surfactants: sucrose esters (laurate or myristate) vs. polysorbate 80. A comprehensive physicochemical characterization indicated no significant influence of the solubilized nonsteroidal anti-inflammatory drug on the bicontinuous structure of blank formulations. To evaluate skin tolerability of isopropyl alcohol, a sucrose ester–based microemulsion containing transcutol P as a cosurfactant was also developed. The measured skin parameters strongly depended on the (co)surfactant type, showing higher compatibility of the microemulsions containing sucrose ester and isopropyl alcohol. *In vitro* release results, *in vivo* tape stripping and pharmacokinetics in rats confirmed superiority of the sucrose ester– over polysorbate–based microemulsions (total amounts of aceclofenac penetrated 60.81 ± 5.97 and 60.86 ± 3.67 vs. 27.00 ± 5.09 μg/cm^2, and its maximum plasma concentrations 275.57 ± 109.49 and 281.31 ± 76.76 vs. 150.23 ± 69.74 ng/ml for sucrose laurate– and myristate– vs. polysorbate 80–based microemulsions, respectively). Hence, sugar–based excipients increased delivery of aceclofenac through *stratum corneum* by increasing its fluidity, showing overall more satisfying safety profiles. In conclusion, sucrose ester–based microemulsions proved to be promising carriers for dermal/transdermal aceclofenac delivery.

Keywords: Bicontinuous microemulsion; Sucrose ester; Aceclofenac; Skin irritation potential; Tape stripping; Pharmacokinetics

1. Introduction

Aceclofenac (AC) is an orally effective nonsteroidal anti-inflammatory drug (NSAID), indicated for use in patients with osteoarthritis, rheumatoid arthritis and ankylosing spondylitis, as well as for the symptomatic therapy of pain and inflammation (Jana et al., 2013). Although efficacious and relatively safe, chronic oral AC administration may cause systemic side effects characteristic for NSAIDs, due to inhibition of prostaglandin synthesis (Raza et al., 2014), which warrants the search for a new route of its administration in the therapy of musculoskeletal disorders. AC has both hydrophobic and hydrophilic properties and log P value close to 2, within an optimal range for candidates for dermal/transdermal delivery following topical application (Beetge et al., 2000; Dave et al., 2015; Heyneman et al., 2000). An ease of application, reduced drug degradation, decreased side effects, avoiding first-pass metabolism and enhanced patient compliance would all be potential benefits of topical over oral AC administration, if the condition of comparable efficacy is fulfilled (Jana et al., 2014; Raza et al., 2014).

The crucial step during any topical NSAID therapy is the drug's ability to overcome the outermost layer of the skin – *stratum corneum* (SC), as the critical barrier for penetration of an active through the skin in sufficiently high amount to exert its clinical effect (Brunner et al., 2011; Changez et al., 2006; Jana et al., 2014; Raza et al., 2014). Consequently, in our research, colloidal carrier systems – microemulsions are introduced as promising vehicles for dermal/transdermal delivery of AC (Al Abood et al., 2013; Naoui et al., 2011; Sahle et al., 2013; Schwarz et al., 2012). They represent a transparent, optically isotropic, thermodynamically stable amphiphile-stabilized dispersion of otherwise two immiscible phases – water and oil (Bardhan et al., 2013). The increased interest in microemulsions stems from their potential benefits over traditional formulations, such as immense interfacial area with corresponding high solubilization capacity, penetration enhancement through the

biological membranes, high stability and ease of preparation (Das and Mitra, 2014; Sahle et al., 2012). Depending on the composition, spontaneous curvature and flexibility of the surfactant film, they can be characterized as water in oil, oil in water or bicontinuous (domains of water and oil co-exist together) systems (Das and Mitra, 2014; Formariz et al., 2008). While the curvature of the surfactant film tends to zero, the interface becomes fluid enough and droplets coalesce during collisions, resulting into equilibrium bicontinuous structure made of interconnected three-dimensional networks of water and oil (Naoui et al., 2011). Such dynamic structures are characterized by a higher amphiphilic character, greater fluctuating interface, a lower interfacial tension and improved solubilizing properties when compared to both globular types of microemulsions (Bhatia et al., 2013; Naoui et al., 2011).

Considering the high concentration of surfactant and/or cosurfactant, the main challenge in topical microemulsion formulation is to effectively increase the penetration of a drug through the SC while avoiding skin irritation (Yuan et al., 2008). Consequently, the choice of components is challenging and, beside their ability to form stable microemulsions, should carefully take into account their biological and pharmaceutical acceptability (Changez et al., 2006; Das and Mitra, 2014). Here, there is a growing interest in using non-ionic surfactants, which are reportedly less toxic and irritant than other types of surfactants, and are commonly classified on the ethylene oxide-based (e.g. polysorbates – P) and polyhydroxy-based (e.g. sucrose esters – SEs) surfactants (Kovacevic et al., 2011; Tadros, 2005). SEs are meant to be nontoxic surfactants obtained from a naturally occurring carbohydrate, with features of low skin sensitization and enhancing skin penetration, as well as with a high environmental compatibility, all of which may be distinct advantages when compared to P, the conventionally used synthetic ethoxylated surfactants (Ayala-Bravo et al., 2003; Schwarz et al., 2012; Szűts and Szabó-Révész, 2012; Tadros et al., 2005).

A detailed introductory analysis of the phase behavior and structural aspects of microemulsion systems, comprising SE, isopropyl alcohol (IPA), isopropyl myristate (IPM) and ultra-purified water, has been recently presented by our group (Todosijević et al., 2014). To extend that study, we used the previously selected biocompatible microemulsions, in order to compare their physicochemical and biopharmaceutical properties, as well as their skin tolerability and ability for dermal/transdermal AC delivery, assessed via *in vivo* penetration study in human volunteers and *in vivo* pharmacokinetic study in rats, with non-ionic microemulsion based on the synthetic surfactant – P. We hypothesized that structural differences in the used surfactants may result in distinctive changes in nanostructure, skin tolerability and penetration-enhancement capability of non-ionic microemulsions. An attempt has also been made to investigate the influence of the chain length of SEs on the measured parameters.

2. Materials and methods

2.1. Materials

AC was purchased from Jinan Jiaquan Chemical Co. Ltd (China). Sucrose laurate D-1216 (SL) and sucrose myristate C-1416 (SM), used as surfactants, were generously donated by Mitsubishi-Kagaku Foods Corporation (Tokyo, Japan). SEs were chosen in such a way that the purity of the main fatty acid (lauric and myristic acid in the case of SL and SM, respectively) equals 95%, they have the same HLB value of 16, ester composition (80% monoester and 20% di-, tri- and polyester) as well as head group, while differ in the tail length. Polysorbate 80 (P80), also used as a surfactant, was obtained from Sigma–Aldrich Laborchemikalien GmbH (Seelze, Germany). IPA (Brenntag, Wien, Austria) and IPM (Comcen, Belgrade, Serbia) were used as a cosurfactant and an oil phase, respectively. Ultra-purified water (GenPure apparatus, TKA Wasseranfbereitungssysteme GmbH, Neiderelbert, Germany) was used as a hydrophilic phase.

2.2. Preparation of AC-unloaded and AC-loaded microemulsions

The pseudo-ternary phase behavior of the system IPM/SE-IPA/ultra-purified water, at fixed surfactant-to-cosurfactant weight ratio 1:1 (K_m), has been described in our previous work with the help of phase diagrams (Todosijević et al., 2014). The current investigation extends our previous study with the comprehensive characterization of the selected SE-based microemulsions, which showed maximum solubilization capacity for AC. For the purpose of the comparison, P80-based microemulsion was also developed, with the same ratio of components (K_m ratio 1:1, and (surfactant + cosurfactant)-to-oil weight ratio 9:1). Briefly, microemulsions were prepared at the room temperature as described: appropriate mass of ultra-purified water (35% *w/w*) was added into mixture of oil and surfactant blend (K_m ratio 1:1) under magnetic stirring. AC was incorporated into prepared microemulsions to give the final concentration of 2% (*w/w*). The given names and composition with the weight ratio of each component of the studied blank formulations are given in Table 1.

2.3.Microemulsion characterization

2.3.1. Polarization microscopy

Microemulsions, as isotropic and transparent systems, do not interfere with the polarized light. Thus, blank and AC-loaded microemulsions were checked for the lack of birefringence (and for the presence of drug crystals) using Motic digital microscope DMB3-223ASC and Motic Images Plus v.2.0 software (Motic GmbH, Wetzlar, Germany).

2.3.2. pH measurements

The pH value of the blank and AC-loaded microemulsions was measured using HI9321 pH meter (Hanna Instruments Inc., Ann Arbor, Michigan). The measurements were performed in triplicate at 25°C.

2.3.3. Electrical conductivity measurements

The electrical conductivity of the samples was measured using CDM230 Conductivity Meter (Radiometer, Copenhagen, Denmark). The measurements were performed in triplicate at 25°C.

2.3.4. Rheological measurements

The rheological behavior of the samples was evaluated using DV-III ULTRA Programmable Rheometer and Rheocalc software v.4.3 (Brookfield Engineering Laboratories, Middlesboro USA), equipped with cone and plate measuring device. The shear stress measurements were performed within the shear rate range from 375 to 1875 s^{-1}, and back to the start point, at 20 ± 1°C.

2.3.5. Differential Scanning Calorimetry (DSC)

DSC investigation was performed using Mettler Toledo DSC 1, STAR^e System (Mettler Toledo GmbH Analytical, Giessen, Germany), and thermoanalytical parameters (i.e. enthalpy, onset, and peak temperature) associated with each thermal transition, were obtained by integration of the area of the relevant DSC peaks, using Mettler Toledo STAR^e Software. To evaluate the physical state of AC in microemulsions, the samples were precisely weighted (5 to 10 mg) into 40-µl aluminum pan, hermetically closed, and scanned between 25 to 200°C, at a heating rate of 10°C/min. Additionally, to investigate the microemulsion structure by evaluation of the water behavior, approximately the same amount of the sample was accurately weighted, aluminum pans were hermetically sealed, and DSC curves were generated by cooling the samples from 25 to -60°C, with a cooling rate of 5°C/min. In both investigations, nitrogen with a flow rate of 50 ml/min was used as a purge gas, and an empty sealed aluminum pan was used as a reference.

2.3.6. Thermogravimetric Analysis (TGA)

TGA was introduced in order to better assess the mode of water distribution in the developed microemulsions. Small amount of the sample was placed in an open aluminum pan and heated in Netzsch STA 409PG (Netzsch, Selb, Germany), at a heating rate of 5°C/min, from 25 to 130°C under constant helium flow (40 ml/min).

2.3.7. Fourier Transform Infrared Spectroscopy (FTIR)

For precise evaluation of the chemical interaction among AC and other ingredients, spectral scanning was performed in the wavelength range between 4000 and 400 cm^{-1}, with a BOMEM Hartmann & Braun MB-Series FTIR spectrophotometer (ABB Bomem Inc., Quebec, Canada). The FTIR spectrum of the pure AC was obtained using the potassium bromide pastille method. For microemulsion samples (blank and AC-loaded microemulsions) and for liquid excipients (ultra-purified water, IPM, IPA and surfactant blend), a 10 μL of the sample was placed on the KRS-5 plate. The FTIR spectra of all samples were recorded with a resolution of 4 cm^{-1}, using 10 scans for each spectrum.

2.3.8. Atomic Force Microscopy (AFM)

Morphology of blank and AC-loaded microemulsions was observed using AFM. 48 h prior to the investigation, 10 μL of the sample was directly deposited onto a small, circular mica disc (Highest Grade V1 AFM Mica Discs; Ted Pella Inc., Redding, California) and dried in desiccator. Measurements were performed with NTEGRA prima AFM (NT-MDT, Moscow, Russia) operating in intermittent-contact AFM mode in air. For this purpose, NT-MDT NSGO1 silicon cantilevers (N-type, Antimony doped, Au reflective coating) were used. Nominal force constant of these cantilevers is 5.1 N/m, while their resonance frequency lies in the range 87-230 kHz. During the measurements cantilever driving frequency was 156 kHz, and line scanning frequency was 1 Hz. Both topography and "error signal" AFM images were taken and later analyzed using the software Image Analysis 2.2.0 (NT-MDT, Moscow, Russia).

2.4. In vivo assessment of blank samples' irritation potential

Ten healthy female volunteers (aged 21 – 23), without reported skin diseases or skin lesions, and with no history of allergic reactions, participated in the 24-h study under occlusion after signing the inform consent. Prior to the experiment, the volunteers were informed about the protocol, agreed to participate in the study, and they were asked not to apply any topical products on the forearm up to 24 h prior to the experiment. Signed written consents were obtained in accordance with the Helsinki Declaration and local Ethical Committee.

Taking into account that IPA may cause dry skin, the irritation potential of developed microemulsions (FL, FM and FP) was compared with those which are quantitatively the same, but differ in the type of cosurfactant (named FT, Table 1), as explained in Supplementary material. *In vivo* safety potential of the blank samples FL, FM, FP and FT was assessed via three skin parameters – transepidermal water loss (TEWL), erythema index (EI), and SC hydration (SCH). On the day of experiments, volunteers were instructed to spend 30 min in the study room prior to measurements in order to adapt to room conditions (temperature 23 ± 1°C, relative humidity 35 ± 5%). Afterwards, on the previously delimited test areas, SCH, TEWL, and EI of forearm skin surface were measured using Cutometer® MPA 580, Mexameter® MX18 and Tewameter® TM210, respectively, from Courage Khazaka (Köln, Germany). Two sites were left untreated as controls: non-treated control under occlusion (NCO) and without occlusion (NCWO). After initial measurements, blank microemulsions were applied and covered with 8 mm Finn Chambers® (Smart Practice, Phoenix, Arizona, USA). After 24-h occlusion, the chambers were removed, and 60 min later, all parameters were reassessed on the same position on the flexor aspects of forearms. Parameters are presented as percentage change of the second versus the first day as the baseline.

2.5. In vitro release studies through synthetic membrane

In vitro release profiles were assessed through the previously rehydrated artificial membranes (0.2 μm cellulose membrane, Sartorius, Stedim Biotech GmbH, Göttingen, Germany) mounted on Franz cells with the available diffusion area of 0.785 cm^2. Precise volume (8-9 ml) of the freshly prepared phosphate buffer (pH 7.4) was placed in the receiver compartment and magnetically stirred at 300 rpm. The accurately weighted AC-loaded formulation (400-420 mg) was placed on the cellulose membrane in the donor chamber, taking care to avoid incorporation of air bubbles which limit the diffusion of drug. Franz cells were mounted in a water bath at 37°C, while the temperature of the membranes was 32°C. Aliquots of 500 μl of the acceptor medium were collected from the receiver cell at regular time intervals over 6 h (the sampling was performed at 0.5, 1, 1.5, 2, 3, 4, 5 and 6 h) and filtrated using 0.45 μm MF-Millipore® membrane filter (Millipore Corporation, Bedford, USA). In order to maintain sink conditions, each aliquot was replaced with the same volume of the fresh preheated medium. AC concentration was determined using high performance liquid chromatography (HPLC, Dionex, UltiMate 3000 Thermo Scientific, Germering, Germany): 20 μl of the sample was injected through a partial loop, separations were performed on a Luna C18 column (100 A, 250 mm x 4.6 mm, 5 μm), whereas the mobile phase consisted of acetonitrile/methanol/0.5% *w/v* ammonium acetate (pH = 5.9) (27/18/55). The flow rate of the mobile phases was 1 ml/min, and the column temperature was set at 25°C. UV detection was performed at 274 nm. The experiments were carried out in triplicate, and results were plotted as the cumulative released drug percentage versus time. Statistical and model-dependent methods were proposed to compare the obtained drug release profiles. The obtained AC liberation profiles were assessed by fitting experimental data to the mathematical equations describing the following kinetic models: Higuchi, zero order, first order and Korsmeyer-Peppas mathematical models (data available in Supplementary Material). Linear regression analysis

was performed, and the model which gave the highest correlation coefficient (R^2) value was considered to be the most suitable kinetic model for describing the release of AC from the investigated systems.

2.6. In vivo skin absorption assessment – tape stripping method

Three healthy females (aged 23 – 26), who had no history of skin diseases or allergic reactions, participated in the study after signing the inform consent. On the day of experiments, volunteers were instructed to spend 30 min in the study room prior to measurements in order to adapt to room conditions. All samples were uniformly applied topically, on the intact skin areas previously delineated using a permanent marker pen to ensure that the SC layers were removed throughout the experiment on the same position. After a residence time of 1 h, which is the application time selected based on the similar works (Mahrhauser et al., 2014; Schwarz et al., 2013; Teichmann et al., 2007), SC layers were removed using twelve adhesive D-squam® tapes with surface area of 3.8 cm^2. After applying the uniform pressure of 140 g/cm^2 for 10 s, each tape was stripped rapidly in a single movement. TEWL proved as a useful parameter in the assessment of the functional state of the skin barrier, and therefore it was measured at the baseline, after 7th and the last (12th) tape. Additionally, measurement of TEWL allows normalization of the individual skin thickness, permitting the expression of drug concentration profile ($\mu g/cm^2$) as a function of relative position within the SC (x/L) (Hathout et al., 2011; Jaksic et al., 2012). The apparent thickness of SC (L) was calculated as described elsewhere (Kalia et al., 2001), whereas estimation of the removed SC layer thickness (x), was done by determination of the precise weight of each tape after removal using the equation explained in the work of Jakšić et al. (2012).

The amount of AC was determined in the supernatant, obtained after sonification (Sonorex RK102H, Bandelin, Berlin, Germany) of each tape (first two tapes were discarded) with 5 ml

of ethanol (70% *v/v*) for 15 min, followed with centrifugation (Centrifuge MPW-56, MPW Med. Instruments, Warszawa, Poland) at 4000 rpm for 5 min. Afterwards, samples were filtered through 0.45 μm MF-Millipore® membrane filter and assayed by liquid chromatography–tandem mass spectrometry (LC–MS/MS).

2.7. In vivo pharmacokinetic study in rats

Experiments with animals were conducted in compliance with the EEC Directive 86/609. The protocol was reviewed and approved by the Ethical Committee on Animal Experimentation of the Faculty of Pharmacy, University of Belgrade, Serbia. Male Wistar rats (Military Farm, Belgrade, Serbia) were housed in plastic cages, on a 12-h light-dark cycle, with free access to pellet food and tap water. The temperature of the animal room was 22 ± 1°C, the relative humidity 40–70%, and the illumination 120 lx.

Briefly, the rats were divided into 5 groups and treated as follows:

Group 1: topical application of 200 μl of AC-loaded SL-based microemulsion (FLAc);

Group 2: topical application of 200 μl of AC-loaded SM-based microemulsion (FMAc);

Group 3: topical application of 200 μl of AC-loaded P80-based microemulsion (FPAc);

Group 4: intravenous application of AC solution (25% of ethanol (96% *v/v*) and 75% of the phosphate buffer, pH = 7.4);

Group 5: subcutaneous application of the AC solution.

In the groups intended for topical application (groups 1-3), one day prior the experiment, animals were lightly anesthetized by *i.p.* injection of ketamine (10% Ketamidor, Richter Pharma Ag, Wels, Austria), and hair of the back was shaved and afterwards washed gently with distilled water. On the day of experiment, samples were applied to the shaved region via open containers glued to the skin, delimited to the surface area of 2.01 cm^2. In order to prevent formulation leakage, the containers were tightly covered with the silicone film (Parafilm®, USA). In the group 4 intended for *i.v.* administration (15 mg/kg), AC solution was

infused into the tail vein using a syringe pump (Stoelting Co., Wood Dale, USA), whereas the same dose of the AC solution was injected subcutaneously in the last group of rats.

In all groups, blood samples (200 µL) were collected from the tail vain, at the predetermined time intervals (20 min, 40 min, 60 min, 3 h, 6 h, and 24 h of post-dose) in heparinized tubes. The plasma (100 µL) was separated immediately by centrifugation at 3000 rpm for 15 minutes (Eppendorf MiniSpin® plus centrifuge, Westbury, NY, USA). AC was extracted using the modified procedure by Mutalik et al. (2008), in which 100 µl of rat plasma, 25 µl of methanol and 200 µl of acetonitrile were added to tube, vortexed for 60 s and 675 µl of diluent (methanol and ultra-purified water in the mixture of 80:20 (*v/v*)) was added up to 1 ml. The resulting solution was vortexed for 60 s and centrifuged at 10000 rpm for 10 min. Preparation of calibration standards in plasma was done by addition of 5 µl of the working standard solutions (containing 1, 2, 5, 10, 20, 30, 50 and 70 µg/ml of aceclofenac and the same concentration of diclofenac using methanol) into 95 µl of plasma, followed by the same procedure as described above. Subsequently, the supernatant was separated and analyzed using LC–MS/MS system.

Using Microsoft® Excel–based program PK Functions (Usansky, Desai and Tang-Liu, Department of Pharmacokinetics and Drug Metabolism, Allergan, Irvine, California), the following pharmacokinetic parameters were calculated: the maximum plasma concentration of AC and diclofenac (c_{max} and c^*_{max}, respectively), the time to reach the maximum plasma concentration of AC and diclofenac (t_{max} and t^*_{max}, respectively), and the area under the plasma concentration curve as a function of time, from time zero to the time of the last measured concentration (c_{24}), of AC and diclofenac ($AUC_{0–24}$ and $AUC^*_{0–24}$, respectively).

2.8. LC–MS/MS

LC-MS/MS was used for detection of AC in each stripped sample as well as for detection of AC and diclofenac in rat plasma. Each sample was injected into a Thermo Scientific Accela

600 UPLC system connected to a Thermo Scientific TSQ Quantum Access MAX triple quadrupole mass spectrometer (Thermo Fisher Scientific, San Jose, California) equipped with heated electrospray ionization (HESI) source. XTerra® MS C18 column (2.1 × 150 mm^2, 3.5 µm; Waters Corporation) was used as a column, whereas mobile phase consisted of acetonitrile and 0.1% formic acid (75:25, *v/v*) at a flow rate of 0.5 mL/min. Total analysis time was 2.2 min at temperature 25°C. High-purity nitrogen was used as nebulizing gas in the HESI source. HESI source and MS parameters were as follows: spray voltage 5 kV, vaporizer temperature 400°C, sheath gas pressure 50 units, ion sweep gas 0 units, auxiliary gas 45 units, ion transfer capillary temperature 300°C, capillary offset 15 units, tube lens offset 96 units, skimmer offset 20 units, peak width relating to resolution 0.7 for Q1, scan with (*m/z*) 0.02, scan time 200 ms. Quantification was conducted using selected reactions monitoring in positive scan mode for AC and diclofenac: 353.8→213.9 m/z and 296.0→214.0 m/z, respectively.

2.9. Statistical analysis

Statistical analysis was performed using IBM SPSS® Statistics 19 software (IBM, NY, USA). Statistical analysis of *in vitro* release data was carried out using one-way analysis of variance (ANOVA) followed by Tukey's post hoc test. The parameters from the *in vivo* skin irritation experiments (SCH, EI, TEWL), measured on the second day, were compared to the baseline values using Mann–Whitney U-test. For *in vivo* effects (SCH, EI, TEWL), percentage changes (second versus first day) of the placebo samples were compared mutually and related to the NCWO and NCO, using the one-way ANOVA, followed by either Tukey's or the Games–Howell post hoc test, when p value in Levene's test for homogeneity of variance was greater than 0.05 or below 0.05, respectively. Parameters of *in vivo* tape stripping (total amount of AC penetrated) and pharmacokinetic experiments (c_{max} and $AUC_{0\text{-}24}$) were

assessed with the one-way ANOVA followed by Tukey's post hoc test. Statistical significance was set at $p < 0.05$.

3. Results and discussion

3.1. Physicochemical characterization – determination of microemulsion nanostructure

Incorporation of AC into microemulsions has affected the pH value of each formulation in a similar degree, due to the acidic properties of the drug (Table 2). The pKa value of AC (pKa = 4.7) (Cordero et al., 1997), in parallel with the present experimental results, indicated existence of a large fraction of the unionized drug. This is pertinent, as unionized moiety of a NSAID is expected to contribute to a better skin penetration, thus increasing the bioavailability of the drug, whereas the ionized moiety limits dermal/transdermal permeation due to lower solubility in SC lipids (Beetge et al., 2000; Cordero et al., 1997).

All tested microemulsions showed a linear relationship between shear stress and shear rate (data not shown), demonstrating Newtonian flow behavior with the apparent viscosity values in the range of 16-27 mPa s (Table 2). Very low viscosity, in parallel with the lack of birefringence under polarized light, distinguished these systems from liquid crystalline structures, which possess closely related type and proportion of components (Formariz et al., 2008). While viscosity of a microemulsion vehicle depends on the composition, i.e. water and surfactant content (Ren et al., 2014), and our formulations were selected so that the concentration of components is the same, the viscosity of developed microemulsions apparently depended on the type and structure of surfactant, as shown in Table 2. Viscosity values tended to increase slightly in the case of P80-based microemulsions (FP and FPAc) in comparison to SE-based systems, and this trend followed the increment in the molecular weight of surfactants (524.6, 552.65, 1310 g/mol for SL, SM and P80, respectively). It should be noted that the presented SEs' molecular weights represent the weights of sucrose monolaurate and sucrose monomyristate, which equal 80% of the total surfactant content.

Incorporation of AC slightly affected the viscosity of the microemulsions, but did not change the general flow behavior.

Conductivity values, presented in Table 2, indicated the presence of conductive paths, which are responsible for the conductance of the system (Ustündağ Okur et al., 2014). These values, together with the full study of conductivity behavior along selected water dilution line ((surfactant + cosurfactant)-to-oil weight ratio 9:1), as examined in our former study (Todosijević et al., 2014), suggested bicontinuous structure of the investigated samples. In the microemulsions containing AC, the electrical conductivity increased only slightly in comparison to unloaded formulations, confirming the absence of significant fraction of the ionized drug, which is in line with pKa value of AC and the measured pH values.

The exothermic water peaks at very low temperatures on DSC cooling curves of the samples FL, FM, and FP (Fig. 1) indicated either a bicontinuous or water in oil microemulsion (Bardhan et al., 2013; Sahle et al., 2013). Notably, in the case of water in oil microemulsions, the interactions with the rest of the system profoundly altered thermodynamic properties of water, moving its freezing point to the extremely low temperatures, below the set limit of detection, as also shown in our previous study (Todosijević et al., 2014). These results suggested that hydration of surfactant, in combination with partial miscibility and hence interaction with IPA, is a likely reason for the absence of sharp exothermic peak of ultra-purified water at −6.92°C. Moreover, the peak of bound water on DSC thermograms was slightly moved to the lower temperatures in the case of SL-based (-44.94 and -44.80°C, for FL and FLAc, respectively) in comparison to SM-based systems (-42.37 and -42.82°C for FM and FMAc, respectively). Because of the shorter chain length, and therefore more hydrophilic nature of SL, the binding capability of water was more distinct with respect to SL than to SM, resulting in the freezing peaks at the lower temperatures. Although the addition of a drug into the colloidal carrier system might have affected the nanostructure of the system, due to its

influence on the surfactant film and the interaction between surfactant and vehicle molecules (Junyaprasert et al., 2007; Liu and Chang, 2011), the DSC thermograms did not reveal any significant effect of the solubilized AC on the water behavior.

DSC heating curves are presented in Fig. 2a. The DSC thermogram of pure AC showed an endothermic peak at 152.86°C, corresponding to the melting point of the drug. The broad endothermic peak in the range of approximately 50 to 115°C corresponded to the evaporation of the IPA (onset 78.58°C, peak 82.23°C) and ultra-purified water (onset 98.29°C, peak 103.01°C), which was confirmed by the partial weight loss of the samples over the predefined temperature ranges, detected on the TGA thermograms (data not shown). FTIR spectra of pure AC, blank and AC-loaded microemulsions are shown in Fig. 2b. As presented in Supplementary material, the FTIR spectrum of AC contained peaks consistent with the literature data (Jana et al., 2014; Suresh et al., 2014). Moreover, the bands shown in FTIR spectra of blank microemulsions clearly appeared at the same wavenumbers in the spectra of AC-loaded microemulsions, without any new peaks or potential shifts, suggesting no alteration in the microemulsion structure upon drug incorporation (Hathout et al., 2010). These results, in parallel with DSC heating curves, proved that AC was completely solubilized in the investigated microemulsions, without any drug recrystallization or any chemical interactions among functional groups.

Atomic force micrographs, shown in Fig. 3, represent the structures that can be found in bicontinuous microemulsions with intertwining oil and water phases. In 2D error signal images it can be clearly seen that distinct water droplets are still in contact with each other, further leading to the formation of water clusters and channels which coexist with oil domains. As shown in Fig. 3b, the addition of AC did not significantly influence the vehicles' nanostructure. Hence, physicochemical experimental techniques, together with atomic force micrographs, indicated that the bicontinuous structure of microemulsions is not prone to

further rearrangement induced by incorporation of the drug. Namely, the observed slight changes in some physicochemical parameters (pH and conductivity) were probably related to the intrinsic properties of AC as the model drug (Junyaprasert et al., 2007).

3.2. Microemulsions – skin irritation potential

The one-way ANOVA revealed a significant group effect on all investigated skin parameters: SCH ($F_{(5, 54)} = 29.543$; $p < 0.001$), EI ($F_{(5, 54)} = 10.105$; $p < 0.001$) and TEWL ($F_{(5, 54)} = 6.252$; $p < 0.001$). One hour after occlusion removal, the significant difference for formulations FL and FM, which differ only in the surfactant chain length, could only be observed in the values of SCH (Fig. 4a), compared to baseline, NCO, and NCWO ($p < 0.001$ for all comparisons), without changes in EI and TEWL (Fig. 4b and 4c, respectively). Significant dehydration may be a consequence of high IPA concentration in these samples. However, in the case of P80-based microemulsion, the observed decrease of SCH was far from reaching statistical significance ($p = 0.364$), which can be explained only as an influence of the distinct difference in the structure of surfactant, having in mind the same concentration of IPA in FL, FM and FP samples as well as the same bicontinuous structure of these formulations. Namely, hydroxyl groups of SEs are responsible for stronger hydrogen bonds with water molecules, whereas oxygen in polyethylene glycol binds water much weaker (Kovacevic et al., 2011), and these interactions may be responsible for higher skin dehydration after application of the vehicles which contain SEs as a surfactant. This finding is important as low hydration may result in an improved penetration of actives through SC. On the other hand, FP and FT were the samples showing some irritation potential (Supplementary material), due to the significant increase in EI after occlusion removal vs. baseline ($p < 0.05$ and $p < 0.01$, respectively), whereas the skin tolerability of the formulations FL and FM was acceptable. Additionally, for the former, but not the latter two formulations, TEWL was significantly increased in comparison to the basal values ($p < 0.05$ and $p < 0.01$, respectively), probably indicating alteration in the skin barrier

function. The increase in TEWL values detected after application of the ethoxylated surfactant is in line with the findings of Bárány et al. (2000), and with the fact that SEs, unlike polysorbates, do not remove the cutaneous fat film and are not expected to denature proteins of the skin surface (Bolzinger-Thevenin et al., 1998). Taking together this part of the study, the investigated SE-based samples with SL and SM showed overall satisfying safety profiles, supporting more acceptable skin tolerability of microemulsions based on natural surfactants, than those containing synthetic P80.

3.3. In vitro release study

Considering the total amount of released AC after 6 h, the one-way ANOVA demonstrated a significant group effect ($F_{(2, 6)} = 33.756$; $p = 0.001$). As presented in Fig. 5, significantly higher total percentage of AC was released from SL- and SM-based systems ($p < 0.001$ and $p = 0.014$, respectively) in comparison to the microemulsion with P80 (87.28 ± 4.89 and 70.66 ± 4.46 vs. 53.65 ± 5.62%, respectively). Since all microemulsions have the bicontinuous structure, with the same total concentration of tensides and equal quantity of drug, concentration gradient is not the only factor governing drug release. In addition, the low pH value of all formulations excluded the potential influence of drug ionization on the liberation process. The higher amount of released AC may be a consequence of a slightly lower viscosity of drug-loaded FL and FM formulations (FLAc and FMAc; Table 2), and a release-enhancing effect of SEs, evident in results showing that SEs increase the liberation of poorly water-soluble drugs (Szűts and Szabó-Révész, 2012). Additionally, a significant enhancement ($p = 0.016$) in AC release from sample FLAc, comparing to SM-based microemulsion, was observed (87.28 ± 4.89 vs. 70.66 ± 4.46%, respectively). This tendency correlates well with the higher AC solubility in SL/IPA than in SM/IPA mixture (Todosijević et al., 2014) and with lower viscosity of SL-based microemulsions (Table 2). It can be deduced from these results that the type of surfactant played an important role in the release of AC. The *in vitro*

liberation profiles were also evaluated kinetically, by fitting the experimental data into different order kinetic equations (Table S1), and these results are presented in Supplementary Material (Table S2).

3.4. Tape stripping

Fig. 6a shows the amount of penetrated AC from different formulations, determined on the removed tape strips as a function of the normalized SC depth. The one-way ANOVA revealed a significant group effect on the total amount of AC penetrated into SC ($F_{(2, 6)} = 15.240$; $p = 0.004$), as presented in Fig. 6b. By comparing the respective dermatopharmacokinetic profiles it can be observed that the amount of drug penetrated into SC was significantly higher in the case of SE-based microemulsions in comparison to FPAc ($p < 0.01$ for both comparisons). Due to the same AC concentration in microemulsions, and the absence of drug crystals observable by AFM or polarization microscopy, concentration gradient or thermodynamic activity of the drug cannot be considered as factors responsible for the differences in drug penetration. Therefore, SEs in the samples FLAc and FMAc may have contributed to the increased drug penetration into the SC. Indeed, it was proposed that SEs alter the ordered structure of the intercellular lipid region in the SC by insertion of the hydrocarbon chains between lipophilic tails of the bilayer, as well as by interaction of the sucrose ring with the polar head groups of the skin lipids (Ayala-Bravo et al., 2003; Cázares-Delgadillo et al., 2005; Yang et al., 2002). In line with the observed reduction in the hydration of skin (Fig. 4a), the proposed mechanism might have led to an increase in molecular motion of the SC, and thence an enhanced diffusion of the drug into skin. The results of tape stripping experiment, together with a higher quantity of AC released from SE-based microemulsions (Fig. 5), suggest superiority of both SEs over P as a surfactant in microemulsion formulations for dermal/transdermal AC delivery. With respect to the possible differences between two SEs,

our results did not reproduce the finding on a higher penetration efficacy of surfactant with lauryl hydrophobic chain (Ganem-Quintanar et al., 1998).

3.5.Pharmacokinetic study in rats

Fig. 7a shows the mean plasma concentration–time profiles of AC from microemulsions, whereas Table 3 summarizes the mean pharmacokinetic parameters after administration of the equivalent doses via different administration routes. Following topical application of the microemulsions FLAc and FMAc, the peak plasma concentrations of AC were 275.57 ± 109.49 and 281.31 ± 76.76 ng/ml, respectively, and were reached at 0.44 ± 0.19 and 0.74 ± 0.32 h. Due to the bicontinuous structure of the formulations and the suggested localization of AC (Todosijević et al., 2014), a close contact with skin might have contributed to the direct release of AC, without transfer of AC from inner to continuous phase and then further onto the skin, which may explain a short t_{max} in the case of SE-based microemulsions. Moreover, pH value of formulations indicated the presence of a large fraction of unionized drug, which can dissolve rapidly in the lipids of the SC, thereby facilitating transport by passive diffusion, and hence skin penetration of drugs (Beetge et al., 2000; Cordero et al., 1997). However, despite the same structure and low pH value, AC absorption from sample FPAc was delayed (c_{max} = 150.23 ± 69.74 ng/ml, t_{max} = 2.41 ± 2.70 h). These results, in parallel with a slower AC release from P80-based system (Fig. 5), further indicated that the dermal/transdermal delivery of AC is dependent on the surfactant structure. When comparing the *in vivo* pharmacokinetic data with skin penetration results, a similar trend is observable, confirming both, the action of SEs as penetration enhancers, and superiority of SE-based over P-based microemulsions.

Diclofenac is the major metabolite of AC in rats (Noh et al., 2015). As shown in Fig. 7a and b, concentrations of diclofenac after topical application of AC-loaded microemulsions were higher than those of AC. Additionally, AUC value of diclofenac was more than threefold greater than AUC of AC after s.c. injection. By comparing c_{max} and AUC of AC and

diclofenac (Table 3) after topical administration of microemulsions and s.c application of AC solution, it can be concluded that AC metabolism was more pronounced after topical application, which is accordant with a higher esterase concentration in the epidermal cells and near to hair follicles than in the dermis of rat (Oesch et al., 2014). In addition, the rapid decrease in AC concentration after i.v. and s.c. administration of AC solution (Fig. 7a and b inset) reflected the fast disposition and elimination. Similar values for half-life ($t_{1/2}$) were observed after i.v. and s.c. application (2.77 ± 1.53 and 4.00 ± 0.08 h, respectively). The values of $t_{1/2}$ after topical application of microemulsions could not be precisely calculated from the obtained data, as AC absorption overlapped with its overall elimination. In this situation, drug is in the elimination phase while still being absorbed and $t_{1/2}$ cannot be calculated correctly (El-Laithy et al., 2011).

Absolute bioavailability of AC (F_{abs}) from all tested transdermal formulations was less than 5% (Table 3), which is in accordance with low AUC or F_{abs} values after percutaneous administration of other NSAIDs as well (Brunner et al., 2005; Brunner et al., 2011; Heyneman et al., 2000; Kienzler et al., 2010; Rhee et al., 2013; Toshiaki et al., 1988). Interestingly, F_{abs} following s.c. application of AC was also very low. Relative bioavailability (F_{rel}) of AC was therefore calculated (transdermal vs. s.c. administration), and the values of F_{rel} greater than 30% (Table 3) indicated that AC successfully penetrated the SC and passed epidermis and dermis after application of the SE-based microemulsions. The low absolute bioavailability suggests that both AC and diclofenac possibly accumulated and diffused into deeper tissues rather than in circulation. Kienzler et al. (2010) suggested that intra-articular tissues may act as reservoirs for topically applied NSAIDs, emphasizing that topical application may allow an NSAID to achieve high intra-articular concentrations without high concentration of drug in the bloodstream. Before drawing further conclusions, it is necessary

to examine whether the concentration of AC, delivered via the formulated microemulsions, is locally high enough to have a therapeutic effect in the inflamed musculoskeletal tissues.

4. Conclusion

Microemulsions for topical AC application were successfully developed, using natural SEs and synthetic P as non-ionic surfactants. Indirect (conductivity, DSC) and direct (AFM) characterization techniques proved a bicontinuous structure of all colloidal carrier systems. According to the *in vivo* skin irritation study, the SE-based microemulsion systems containing IPA as a cosurfactant were well-tolerated irrespective of surfactant chain length, whereas the samples FP and FT were associated with a certain degree of irritation, probably related to the presence of P80 and Transcutol P, respectively. The comparable tendencies were observed in the *in vitro* release, *in vivo* tape stripping and *in vivo* pharmacokinetic studies: the presence of SEs improved the rate and extent of release and penetration/absorption of AC. Indeed, the dermatopharmacokinetic profiles and AUC values showed that SEs facilitated the penetration and bioavailability of the drug. The SE-based microemulsions appeared to be superior over the P80-based microemulsion, and such enhanced topical delivery needs to be further tracked by assessing attainable concentrations of AC in musculoskeletal tissues and effectiveness in animal models of inflammation.

5. Acknowledgments

The authors would like to acknowledge the financial support from the Ministry of Education, Science and Technological Development, Republic of Serbia, through Project TR34031, OI175076 and TR32008. The authors are grateful to Mitsubishi-Kagaku Foods Corporation for supplying sucrose esters.

References

Al Abood, R.M., Talegaonkar, S., Tariq, M., Ahmad, F.J., 2013. Microemulsion as a tool for the transdermal delivery of ondansetron for the treatment of chemotherapy induced nausea and vomiting. Colloids Surf. B Biointerfaces 101, 143-151.

Ayala-Bravo, H.A., Quintanar-Guerrero, D., Naik, A., Kalia, Y.N., Cornejo-Bravo, J.M., Ganem-Quintanar, A., 2003. Effects of sucrose oleate and sucrose laureate on in vivo human stratum corneum permeability. Pharm. Res. 20, 1267-1273.

Bárány, E., Lindberg, M., Lodén, M., 2000. Unexpected skin barrier influence from nonionic emulsifiers. Int. J. Pharm. 195, 189-195.

Bardhan, S., Kundu, K., Saha, S.K., Paul, B.K., 2013. Physicochemical investigation of mixed surfactant microemulsions: water solubilization, thermodynamic properties, microstructure, and dynamics. J. Colloid Interface Sci. 411, 152-161.

Beetge, E., du Plessis, J., Müller, D.G., Goosen, C., van Rensburg, F.J., 2000. The influence of the physicochemical characteristics and pharmacokinetic properties of selected NSAID's on their transdermal absorption. Int. J. Pharm. 193, 261-264.

Bhatia, G., Zhou, Y., Banga, A.K., 2013. Adapalene microemulsion for transfollicular drug delivery. J. Pharm. Sci. 102, 2622-2631.

Bolzinger-Thevenin, M.A., Carduner, C., Poelman, M.C., 1998. Bicontinuous sucrose ester microemulsion: a new vehicle for topical delivery of niflumic acid. I. J. Pharm. 176, 39-45.

Brunner, M., Dehghanyar, P., Seigfried, B., Martin, W., Menke, G., Müller, M., 2005. Favourable dermal penetration of diclofenac after administration to the skin using a novel spray gel formulation. Br. J. Clin. Pharmacol. 60, 573-577.

Brunner, M., Davies, D., Martin, W., Leuratti, C., Lackner, E., Müller, M., 2011. A new topical formulation enhances relative diclofenac bioavailability in healthy male subjects. Br. J. Clin. Pharmacol. 71, 852-859.

Cázares-Delgadillo, J., Naik, A., Kalia, Y.N., Quintanar-Guerrero, D., Ganem-Quintanar, A., 2005. Skin permeation enhancement by sucrose esters: a pH-dependent phenomenon. Int. J. Pharm. 297, 204-212.

Changez, M., Varshney, M., Chander, J., Dinda, A.K., 2006. Effect of the composition of lecithin/n-propanol/isopropyl myristate/water microemulsions on barrier properties of mice skin for transdermal permeation of tetracaine hydrochloride: in vitro. Colloids Surf. B Biointerfaces 50, 18-25.

Cordero, J.A., Alarcon, L., Escribano, E., Obach, R., Domenech, J.A., 1997. Comparative study of the transdermal penetration of a series of nonsteroidal antiinflammatory drugs. J. Pharm. Sci. 86, 503-508.

Das, A., Mitra, R.K, 2014. Formulation and characterization of a biocompatible microemulsion composed of mixed surfactants: lecithin and Triton X-100. Coll. Polym. Sci. 292, 635-644.

Dave, V., Paliwal, S., Yadav, S., Sharma, S., 2015. Effect of in vitro transcorneal approach of aceclofenac eye drops through excised goat, sheep, and buffalo corneas. Sci. World J. 2015:432376. doi: 10.1155/2015/432376.

El-Laithy, H.M., Shoukry, O., Mahran, L.G., 2011. Novel sugar esters proniosomes for transdermal delivery of vinpocetine: preclinical and clinical studies. Eur. J. Pharm. Biopharm. 77, 43-55.

Formariz, T.P., Chiavacci, L.A., Sarmento, V.H., Franzini, C.M., Silva-Jr., A.A., Scarpa, M.V., Santilli, C.V., Egito, E.S., Oliveira, A.G., 2008. Structural changes of biocompatible neutral microemulsions stabilized by mixed surfactant containing soya phosphatidylcholine and their relationship with doxorubicin release. Colloids Surf. B Biointerfaces 63, 287-295.

Ganem-Quintanar, A., Quintanar-Guerrero, D., Falson-Rieg, F., Buri, P., 1998. Ex vivo oral mucosal permeation of lidocaine hydrochloride with sucrose fatty acid esters as absorption enhancers. Int. J. Pharm. 173, 203-210.

Hathout, R.M., Woodman, T.J., Mansour, S., Mortada, N.D., Geneidi, A.S., Guy, R.H., 2010. Microemulsion formulations for the transdermal delivery of testosterone. Eur. J. Pharm. Sci. 40, 188-196.

Hathout, R.M., Mansour, S., Geneidi, A.S., Mortada, N.D., 2011. Visualization, dermatopharmacokinetic analysis and monitoring the conformational effects of a microemulsion formulation in the skin stratum corneum. J. Colloid Interface. Sci. 354, 124-130.

Heyneman, C.A., Lawless-Liday, C., Wall, G.C., 2000. Oral versus topical NSAIDs in rheumatic diseases: a comparison. Drugs 60, 555-574.

Hirata, K., Mohammed, D., Hadgraft, J., Lane, M.E., 2014. Influence of lidocaine hydrochloride and penetration enhancers on the barrier function of human skin. Int. J. Pharm. 477, 416-420.

Jaksic, I., Lukic, M., Malenovic, A., Reichl, S., Hoffmann, C., Müller-Goymann, C., Daniels, R., Savic, S., 2012. Compounding of a topical drug with prospective natural surfactant-stabilized pharmaceutical bases: physicochemical and in vitro/in vivo characterization--a ketoprofen case study. Eur. J. Pharm. Biopharm. 80, 164-175.

Jana, S., Das, A., Nayak, A.K., Sen, K.K., Basu, S.K., 2013. Aceclofenac-loaded unsaturated esterified alginate/gellan gum microspheres: in vitro and in vivo assessment. Int. J. Biol. Macromol. 57, 129-137.

Jana, S., Manna, S., Nayak, A.K., Sen, K.K., Basu, S.K., 2014. Carbopol gel containing chitosan-egg albumin nanoparticles for transdermal aceclofenac delivery. Colloids Surf. B Biointerfaces 114, 36-44.

Junyaprasert, V.B., Boonme, P., Songkro, S., Krauel, K., Rades, T., 2007. Transdermal delivery of hydrophobic and hydrophilic local anesthetics from o/w and w/o Brij 97-based microemulsions. J. Pharm. Pharm. Sci. 10, 288-298.

Kalia, Y.N., Alberti, I., Naik, A., Guy, R.H., 2001. Assessment of topical bioavailability in vivo: the importance of stratum corneum thickness. Skin Pharmacol Phys. 14, 82-86.

Kienzler, J.L., Gold, M., Nollevaux, F., 2010. Systemic bioavailability of topical diclofenac sodium gel 1% versus oral diclofenac sodium in healthy volunteers. J. Clin. Pharmacol. 50, 50-61.

Kovacevic, A., Savic, S., Vuleta, G., Müller, R.H., Keck, C.M., 2011. Polyhydroxy surfactants for the formulation of lipid nanoparticles (SLN and NLC): effects on size, physical stability and particle matrix structure. Int. J. Pharm. 406, 163-172.

Liu, C.H., Chang, F.Y., 2011. Development and characterization of eucalyptol microemulsions for topic delivery of curcumin. Chem. Pharm. Bull. 59, 172-178.

Mahrhauser, D., Hoppel, M., Schöll, J., Binder, L., Kählig, H., Valenta, C., 2014. Simultaneous analysis of skin penetration of surfactant and active drug from fluorosurfactant-based microemulsions. Eur. J. Pharm. Biopharm. 88, 34-39.

Mutalik, S., Manoj, K., Reddy, M.S., Kushtagi, P., Usha, A.N., Anju, P., Ranjith, A.K., Udupa, N., 2008. Chitosan and enteric polymer based once daily sustained release tablets of aceclofenac: in vitro and in vivo studies. AAPS PharmSciTech. 9, 651-659.

Naoui, W., Bolzinger, M.A., Fenet, B., Pelletier, J., Valour, J.P., Kalfat, R., Chevalier, Y., 2011. Microemulsion microstructure influences the skin delivery of an hydrophilic drug. Pharm Res. 28, 1683-1695.

Noh, K., Shin, B.S., Kwon, K.I., Yun, H.Y., Kim, E., Jeong, T.C., Kang, W., 2015. Absolute bioavailability and metabolism of aceclofenac in rats. Arch. Pharm. Res. 38, 68-72.

Oesch, F., Fabian, E., Guth, K., Landsiedel, R., 2014. Xenobiotic-metabolizing enzymes in the skin of rat, mouse, pig, guinea pig, man, and in human skin models. Arch. Toxicol. 88, 2135-2190.

Raza, K., Kumar, M., Kumar, P., Malik, R., Sharma, G., Kaur, M., Katare, O.P., 2014. Topical delivery of aceclofenac: challenges and promises of novel drug delivery systems. Biomed. Res. Int. 2014:406731. doi: 10.1155/2014/406731.

Ren, Q., Deng, C., Meng, L., Chen, Y., Chen, L., Sha, X., Fang, X., 2014. In vitro, ex vivo, and in vivo evaluation of the effect of saturated fat acid chain length on the transdermal behavior of ibuprofen-loaded microemulsions. J. Pharm. Sci. 103, 1680-1691.

Rhee, Y.S., Nguyen, T., Park, E.S., Chi, S.C., 2013. Formulation and biopharmaceutical evaluation of a transdermal patch containing aceclofenac. Arch. Pharm. Res. 36, 602-607.

Sahle, F.F., Metz, H., Wohlrab, J., Neubert, R.H., 2012. Polyglycerol fatty acid ester surfactant-based microemulsions for targeted delivery of ceramide AP into the stratum corneum: formulation, characterisation, in vitro release and penetration investigation. Eur. J. Pharm. Biopharm. 82, 139-150.

Sahle, F.F., Metz, H., Wohlrab, J., Neubert, R.H., 2013. Lecithin-based microemulsions for targeted delivery of ceramide AP into the stratum corneum: formulation, characterizations, and in vitro release and penetration studies. Pharm. Res. 30, 538-551.

Schwarz, J.C., Klang, V., Hoppel, M., Mahrhauser, D., Valenta, C., 2012. Natural microemulsions: formulation design and skin interaction. Eur. J. Pharm. Biopharm. 81, 557-562.

Schwarz, J.C., Hoppel, M., Kählig, H., Valenta, C., 2013. Application of quantitative (19) F nuclear magnetic resonance spectroscopy in tape-stripping experiments with natural microemulsions. J. Pharm. Sci. 102, 2699-2706.

Suresh, S., Gunasekaran, S., Srinivasan, S., 2014. Studies of the molecular geometry, vibrational spectra, frontier molecular orbital, nonlinear optical and thermodynamics properties of aceclofenac by quantum chemical calculations. Spectrochim. Acta A Mol. Biomol. Spectrosc. 125, 239-251.

Szűts, A., Szabó-Révész, P., 2012. Sucrose esters as natural surfactants in drug delivery systems--a mini-review. Int. J. Pharm. 433, 1-9.

Tadros, T.F., 2005. Applied Surfactants—Principles and Applications, Wiley VHC, Weinheim.

Teichmann, A., Heuschkel, S., Jacobi, U., Presse, G., Neubert, R.H., Sterry, W., Lademann, J., 2007. Comparison of stratum corneum penetration and localization of a lipophilic model drug applied in an o/w microemulsion and an amphiphilic cream. Eur. J. Pharm. Biopharm. 67, 699-706.

Toshiaki, N., Akira, K., Kiyoshi, S., Koichi, T., Koichi, M., Kazuhiko, S., Yujin, T., Masaharu, K., Tateo, M., Nobuo, T., 1988. Percutaneous absorption of diclofenac in rats and humans: aqueous gel formulation. Int. J. Pharm. 46, 1-7.

Todosijević, M.N., Cekić, N.D., Savić, M.M., Gašperlin, M., Ranđelović, D.V., Savić, S.D., 2014. Sucrose ester-based biocompatible microemulsions as vehicles for aceclofenac as a model drug: formulation approach using D-optimal mixture design. Colloid Polym. Sci. 292, 3061-3076.

Ustündağ Okur, N., Yavaşoğlu, A., Karasulu, H.Y., 2014. Preparation and evaluation of microemulsion formulations of naproxen for dermal delivery, Chem. Pharm. Bull. 62, 135-143.

Yang, J.H., Kim, Y.I., Kim, K.M., 2002. Preparation and evaluation of aceclofenac microemulsion for transdermal delivery system. Arch. Pharm. Res. 25, 534-540.

Yuan, J.S., Ansari, M., Samaan, M., Acosta, E.J., 2008. Linker-based lecithin microemulsions for transdermal delivery of lidocaine. Int. J. Pharm. 349, 130-143.

Figure Captions

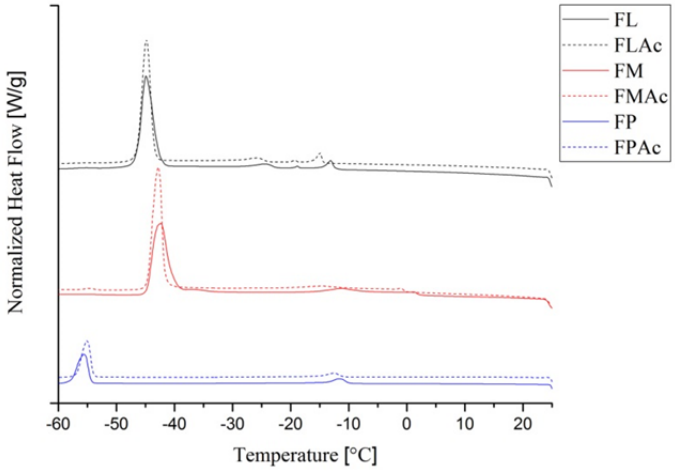

Fig. 1. DSC cooling curves of AC-unloaded and AC-loaded microemulsions.

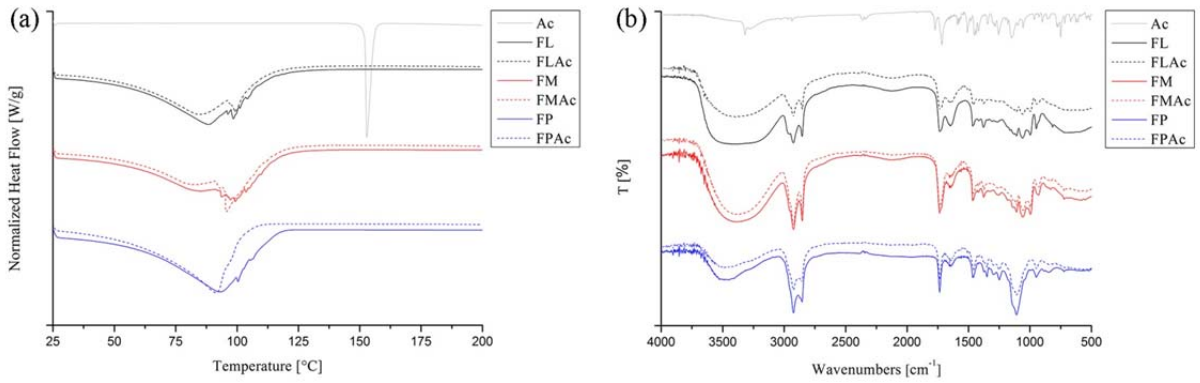

Fig. 2. (a) DSC thermograms and **(b)** FTIR spectra of pure AC, AC-unloaded and AC-loaded microemulsions.

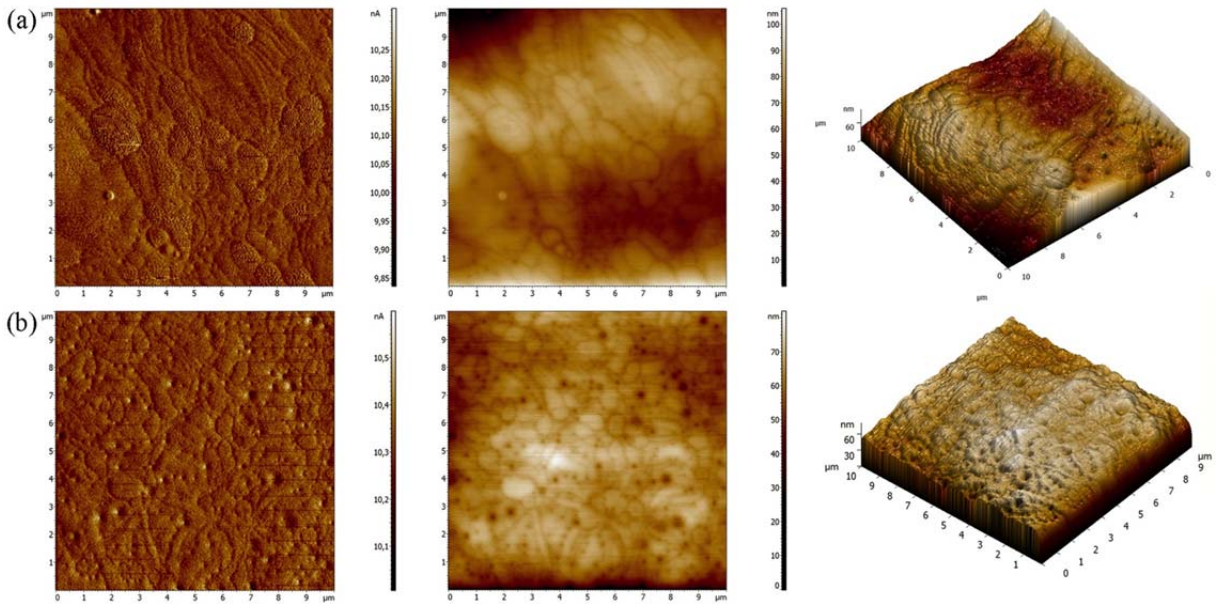

Fig. 3. AFM 2D error signal, 2D and 3D topography images showing the structures of the samples: **(a)** FL, and **(b)** FLAc.

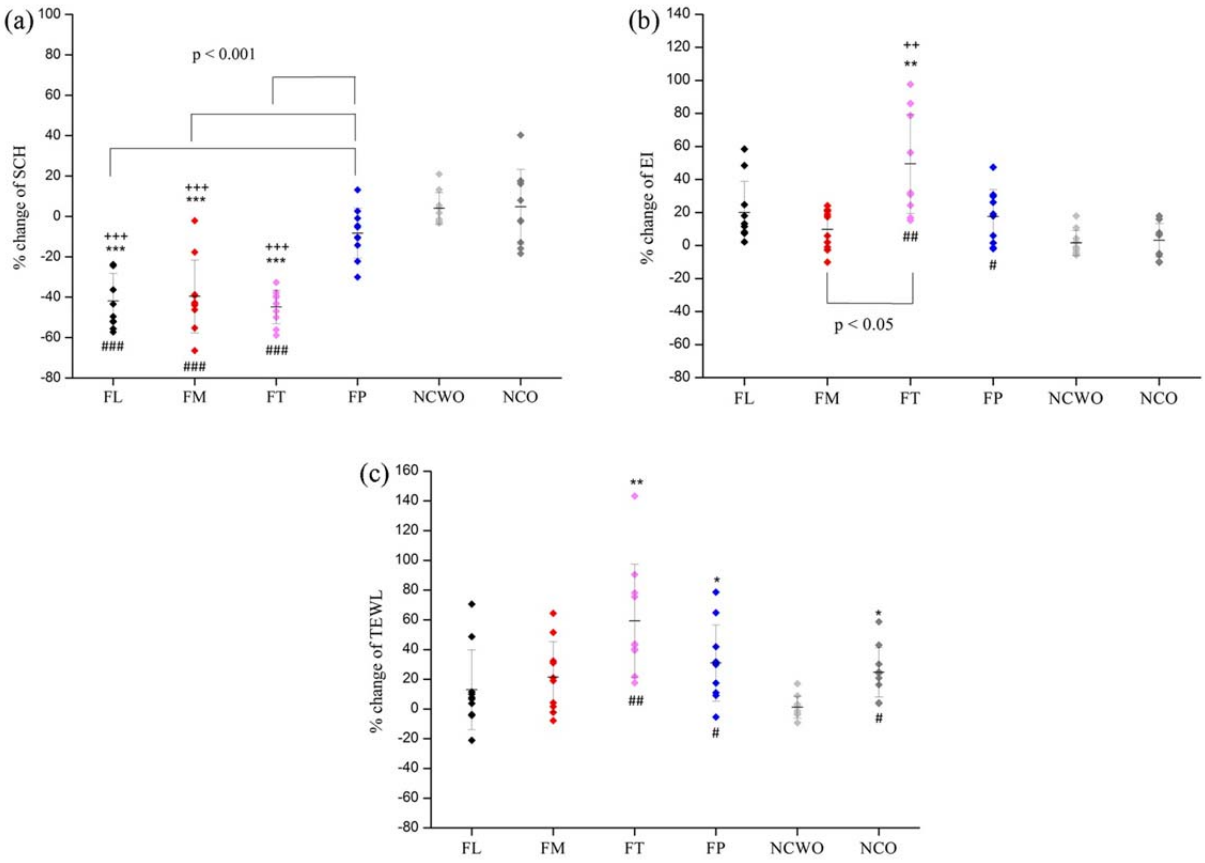

Fig. 4. *In vivo* safety assessment – percentage change in **(a)** *stratum corneum* hydration (SCH), **(b)** erythema index (EI), and **(c)** transepidermal water loss (TEWL) of the skin, after occlusion removal vs. baseline measurements, for investigated placebo samples, non-treated control without (NCWO) and under occlusion (NCO). **(a)** $^{###}p < 0.001$ values after occlusion removal compared to the basal values; ***p < 0.001 % change of SCH of placebo samples compared to the NCWO; $^{+++}p < 0.001$ % change of SCH of placebo samples compared to the NCO; **(b)** $^{#}p < 0.05$ and $^{##}p < 0.01$ values after occlusion removal compared to the basal values; **p < 0.01 % change of EI of placebo samples compared to the NCWO; $^{++}p < 0.01$ % change of EI of placebo samples compared to the NCO; **(c)** $^{#}p < 0.05$ and $^{##}p < 0.01$ values after occlusion removal compared to the basal values; *p < 0.05 and **p < 0.01 % change of TEWL of placebo samples compared to the NCWO. Bold line and whiskers represent the mean value ± SD.

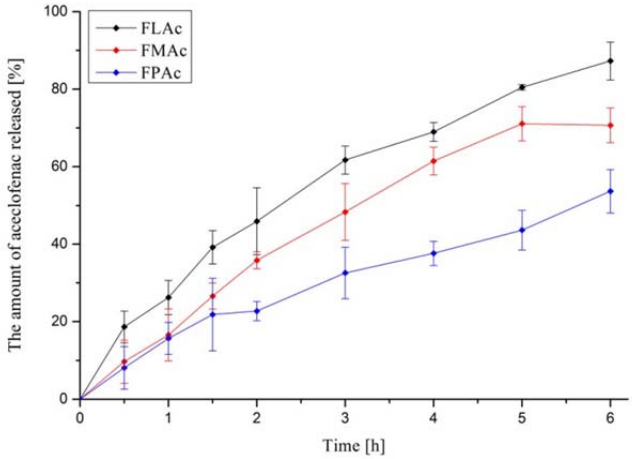

Fig. 5. The release profiles of AC from microemulsions. Data represent the mean value ± SD.

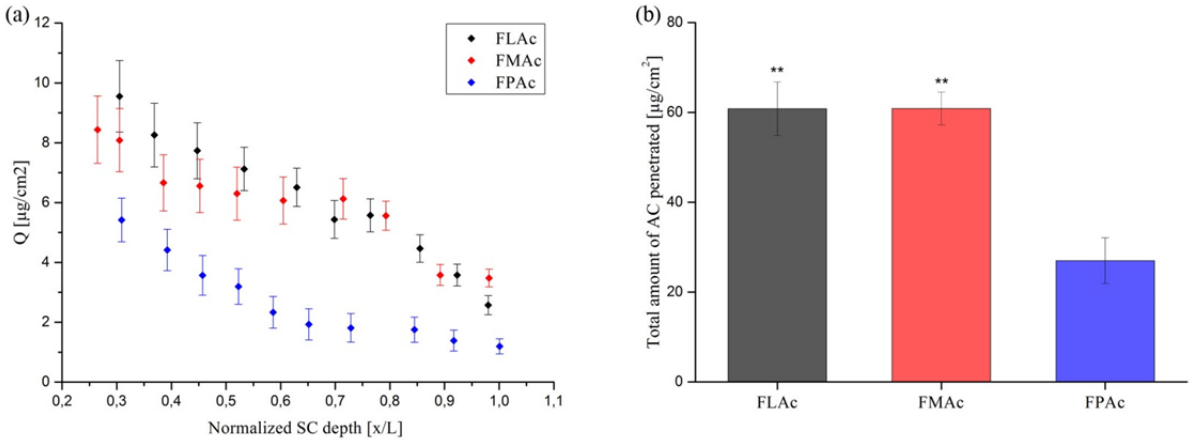

Fig. 6. (a) Comparative penetration profiles of AC from microemulsions assessed through tape stripping technique across the SC path-length L; **(b)** Total amount of AC penetrated from microemulsions. **$p < 0.01$ compared to FPAc. Data represent mean ± SEM.

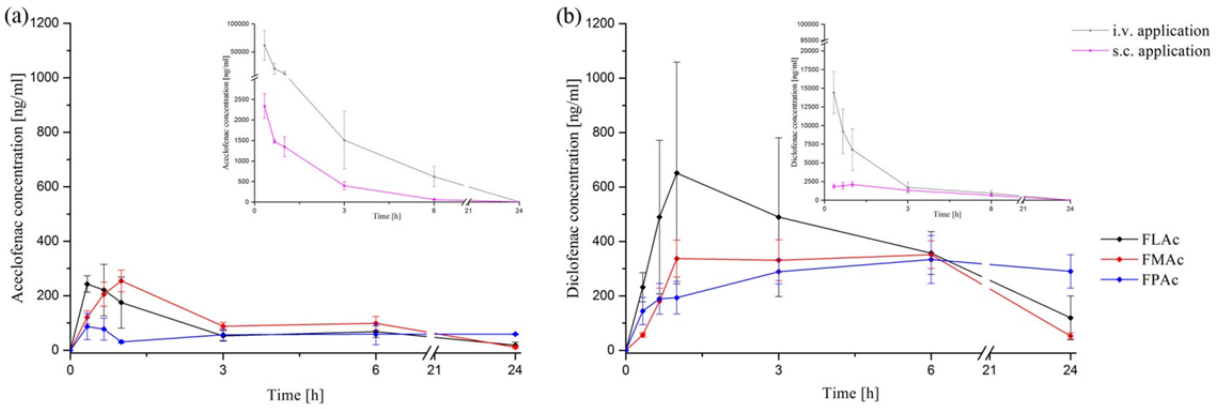

Fig. 7. (a) AC plasma concentration–time profiles of microemulsions after topical application. *Inset*: AC plasma concentration–time profiles after intravenous and subcutaneous application of AC solution; **(b)** Diclofenac plasma concentration–time profiles of microemulsions after topical application. *Inset*: Diclofenac plasma concentration–time profiles after intravenous and subcutaneous application of AC solution. Data represent average of three to five trials ± SEM.

Tables

Table 1. Composition of microemulsion formulations.

Microemulsion composition (%, *w/w*)	FL	FM	FP	FT
Sucrose laurate/Isopropyl alcohol*	58.5			
Sucrose myristate/Isopropyl alcohol*		58.5		
Polysorbate 80/Isopropyl alcohol*			58.5	
Sucrose myristate/Transcutol P*				58.5
Isopropyl myristate	6.5	6.5	6.5	6.5
Ultra-purified water	35.0	35.0	35.0	35.0

*Surfactant-to-cosurfactant weight ratio 1:1.

Table 2. Electrical conductivity, viscosity and pH values of AC-unloaded and AC-loaded microemulsions. Data represent the mean value ± SD.

Formulations	AC-Unloaded Microemulsions			AC-Loaded Microemulsions		
	Conductivity [μs/cm]	Viscosity [mPa s]	pH	Conductivity [μs/cm]	Viscosity [mPa s]	pH
FL	58.13 ± 0.21	16.87*	6.48 ± 0.01	63.9 ± 0.10	18.31*	3.38 ± 0.01
FM	50.50 ± 0.82	19.88*	6.32 ± 0.02	56.83 ± 0.21	19.62*	3.22 ± 0.01
FP	23.10 ± 0.1	26.81*	7.59 ± 0.01	29.47 ± 0.15	26.42*	4.01 ± 0.01

*The apparent viscosity values at the shear rate of 375 s^{-1}.

Table 3. Pharmacokinetic parameters from the plasma concentration-time curves.

	Application route				
	Topical			Subcutaneous	Intravenous
	FLAc	FMAc	FPAc		
c_{max} [ng/ml]	275.57 ± 109.49	281.31 ± 76.76	150.23 ± 69.74	2341.74 ± 593.72	69231.37 ± 68716.47
t_{max} [h]	0.44 ± 0.19	0.74 ± 0.32	2.41 ± 2.70	0.33 ± 0.00	0.00 ± 0.00
AUC_{0-24} [ngh/ml]	1368.77 ± 619.58	1762.56 ± 656.55	1118.65 ± 838.83	4557.54 ± 1360.63	76431.63 ± 72634.09
F_{abs} [%]	1.82	2.35	1.49	6.08	/
F_{rel} [%]	30.62	39.43	25.03	/	/
c^*_{max} [ng/ml]	684.08 ± 676.14	369.12 ± 131.91	371.05 ± 139.31	2374.11 ± 723.42	14408.96 ± 5613.66
t^*_{max} [h]	2.67 ± 2.89	4.00 ± 2.45	9.75 ± 9.60	0.75 ± 0.32	0.33 ± 0.00
AUC^*_{0-24} [ngh/ml]	7051.88 ± 3378.72	5465.67 ± 1755.88	7169.57 ± 3177.83	14245.90 ± 5139.21	39633.45 ± 26878.04
F^*_{abs} [%]	7.39	6.35	7.28	16.52	/
F^*_{rel} [%]	45.66	39.20	44.95	/	/

c_{max}, Peak plasma concentration of aceclofenac; t_{max}, Time of aceclofenac peak plasma concentration; AUC, Area under the curve of aceclofenac; F_{abs}, Absolute bioavailability; F_{rel}, Relative bioavailability (transdermal vs. subcutaneous administration); c^*_{max}, Peak plasma concentration of diclofenac; t^*_{max}, Time of diclofenac peak plasma concentration; AUC^*, Area under the curve of diclofenac; F^*_{abs}, Absolute bioavailability of total aceclofenac and diclofenac concentrations; F^*_{rel}, Relative bioavailability of total aceclofenac and diclofenac concentrations (transdermal vs. subcutaneous administration). Results are expressed as the mean value ± SD.